Single-Phase Mixed Molybdenum-Tungsten Carbides: Synthesis, Characterization and Catalytic Activity for Toluene Conversion

*Ali Mehdad, Rolf E. Jentoft,[§] and Friederike C. Jentoft[§,]**

School of Chemical, Biological & Materials Engineering
University of Oklahoma, Norman, OK 73019, USA

[§]present address: Department of Chemical Engineering, University of Massachusetts, 159 Goessmann Laboratory, 686 North Pleasant Street, Amherst, MA 01003-9303,
* Author to whom correspondence should be addressed: Email fcjentoft@umass.edu

Abstract

A series of single-phase mixed metal carbides of molybdenum and tungsten ($Mo_{2-x}W_xC$, $0 < x < 2$) was synthesized. Precursors with intimately mixed metals were prepared by flash-freezing aqueous solutions of molybdenum and tungsten salts in liquid nitrogen and subsequent freeze-drying. The powders of freeze-dried samples had small particles that facilitated reduction and carburization. Direct carburization of freeze-dried precursors at a final temperature of 650 °C resulted in formation of single-phase metal carbides with hexagonal structures and CO adsorption capacities of 15 to 27 μmol/g. All carbides were catalytically active for conversion of toluene at a total pressure of 21 bar, and a H_2:toluene molar ratio of 33. At a reaction temperature of 250 °C, only methylcyclohexane formed at TOFs of 0.13 ($W_{1.5}Mo_{0.5}C$) – 2.1 s^{-1} (Mo_2C). Activation energies for ring hydrogenation were in the range of 40-60 kJ/mol. At 400 °C, catalysts deactivated for 24 h before stabilizing. At steady state, methylcyclohexane and small alkanes formed via ring hydrogenation and hydrogenolysis, indicating sites with metallic character. Disproportionation of toluene to benzene and xylenes indicated weakly acidic sites. An excess of benzene was attributed to the presence of carbon vacancies on the surface, which formed more readily in the tungsten-containing carbides.

Keywords: Carbide solid solutions, Thermal analysis, X-ray diffraction, Aromatics hydrogenation, Selectivity, Structure sensitivity.

1 Introduction

Transition metal carbides have remarkable catalytic properties, which have been rationalized by electronic structure considerations. Insertion of carbon into the lattice of early transition metals changes the *d* band structure of the metal such that the catalytic activity of metal carbides becomes similar in nature to those of noble metals [1,2]. In addition to catalytic functions typical of metals, carbide surfaces can be modified to exhibit acidic properties. Consequently, reactions catalyzed by metal carbides include hydrogenation [3,4], hydrogenolysis [5] and isomerization [6-9].

Transition metal carbides have profound metallic characteristics. The catalytic behavior of Mo_2C, the most commonly investigated carbide, in the hydrogenation of aromatics illustrates the similarity to noble metals. Adsorption of hydrogen on the surface of Mo_2C can be both atomic (with low energy barrier) and molecular [10] and is stronger than adsorption of hydrogen on the surface of noble metals [11]. Benzene can be hydrogenated on Mo_2C, but the mechanism is unclear; both, an Eley-Rideal mechanism [12,13], and a Langmuir-Hinshelwood mechanism have been proposed [14]. Temperature-programmed desorption of benzene from the surface of Mo_2C was reported to be similar to desorption from ruthenium, with benzene desorption peaks at 104 and 111 ºC from the surfaces of Mo_2C and Ru, respectively [15]. The heat of adsorption of carbon on the surface of Mo_2C and noble metals such as ruthenium was reported to be comparable [11].

The properties of transition metal carbides can be altered by partial substitution of the anions or the cations. A common approach is the chemisorption of oxygen on the surface of metal carbides, which attenuates the metallic properties, that is, the presence of oxygen weakens adsorption of carbon [11] and decreases the hydrogenation and hydrogenolysis activity [4,6,16], while it adds acid functionality [6,17]. However, at temperatures higher than 300 °C, oxygen can be removed from the surface of Mo_2C [16], which changes surface composition and consequently changes the catalytic activity of Mo_2C. One solution to retain oxygen on the surface and to moderate the metallic characteristics of Mo_2C is to add another metal with lower hydrogenation activity and higher oxophilicity.

While there are many papers published about the synthesis and catalytic behavior of mono-metallic carbides, not many exist about bi-metallic carbides. In particular, performance-composition relationships for mixed metal carbides are lacking, because it has proven difficult to

synthesize complete series of single-phase mixed metal carbides without carbon contamination on the surface. Partial success has been achieved by combining molybdenum with neighbors in the periodic table that are slightly more difficult to reduce, for example, niobium [18, 19] and tungsten [20-22]. Both carbides and oxycarbides of these combinations have been synthesized and investigated. Recently, the application of new synthesis routes has expanded the compositional range of Mo-Nb carbides [18]. In contrast, efforts regarding Mo-W carbides have focused on fixed metal ratios [20,23], on high carburization temperatures that resulted in molybdenum enrichment on the surface and low surface areas [21], or on analysis of the surface properties without confirmation of the bulk structure [22]. Research to improve the synthesis methods is thus needed.

High-surface area carbides are most often synthesized by temperature-programmed reduction of oxidic precursors [24], and successful synthesis of single-phase bimetallic carbides hinges on a precursor with intimately mixed metals. Various methods have been used for the synthesis of precursors containing mixed metals prior to carburization, such as physical mixing and fusing of metal oxides [23,25-28], co-precipitation [21,22,29,30], hydrothermal synthesis [18] and flash-freezing followed by freeze-drying (FD) [18]. To avoid a gaseous carbon source, some authors suggested decomposing a mixture containing the metals and a carburization agent such as hexamethylenetetramine [34,35], sugar [36], or urea [37,38]. Among all of the listed methods, the freeze-drying method has the advantages of fully adjustable composition independent of metal chemistries and precursor homogeneity. Flash-freezing followed by freeze-drying has previously been used for the synthesis of oxynitrides [31-33].

This paper describes the first synthesis of a series of molybdenum-tungsten carbides using the freeze-drying method. Solid solutions of carbides over a wide range of metal ratios make it possible to investigate the effect of composition on catalytic activity. Tungsten carbide has lower hydrogenation activity and higher oxophilicity as compared to molybdenum carbide [16]. Molybdenum-tungsten carbides were synthesized before and were tested for dehydrogenation and hydrogenolysis reactions, and mixed molybdenum-tungsten carbides showed higher rates for dehydrogenation than hydrogenolysis as compared to their mono-metallic counterparts [21,39]. Toluene conversion serves as a probe for sites capable of ring hydrogenation, hydrogenolysis, disproportionation and dealkylation.

2 Experimental section

2.1 Catalyst synthesis and monitoring of treatments by thermal analysis

2.1.1 Synthesis of mixed molybdenum-tungsten precursors by flash-freezing

Appropriate amounts of ammonium paratungstate (APT) (Alfa Aesar) and ammonium heptamolybdate (AHM) (ACS reagent, 81-83% MoO_3, Sigma Aldrich) were dissolved separately in water, and the solutions were mixed together to obtain molybdenum molar fractions (metals basis $x_{Mo}= n_{Mo}/(n_{Mo}+n_W)$) of 0, 0.25, 0.5, 0.75, or 1. A total of 1 g of the starting salts was used and water in the amount to obtain a final total metal concentration of 0.1 M. The solution was stirred for 15 min and flash-frozen by adding droplets into liquid N_2. Globules of the frozen solution were recovered, and freeze-dried at a pressure of 110 µtorr in an ATR FD3.0 freeze-drier for 1 day. The obtained solids will be referred to as FD-AHM and FD-APT, or mixtures thereof.

2.1.2 Thermobalance apparatus and gases used for thermal treatments

Thermal treatments of samples were carried out in a thermogravimetric analyzer (TGA) connected to an online mass spectrometer (MS) (Netzsch STA 449 F1 and QMS 403 C Aëolos) via a quartz-glass capillary. Temperature-programmed-reaction experiments were run with an empty crucible to correct for any changes in gas densities and flow rates during the experiment. MS signals were normalized to initial sample mass, which ranged from 88 to 500 mg. Air (zero grade, Airgas) and H_2 (ultra-high purity, Airgas) were passed through a moisture trap (Agilent, MT400-2), and argon (ultra-high purity, Airgas) was passed through dual moisture and oxygen trap (Z-Pure Dual Purifier). Methane (UHP, Airgas) and ethane (99.95%, Matheson) were used as received. Flow rates were adjusted by using flow controllers and are given at STP.

2.1.3 Generation of oxides by calcination of selected precursors

Three of the freeze-dried precursors, with molar ratios of Mo:W= 0:1, 1:0 and 1:1 were calcined in the TG-MS apparatus in 80% air in argon with a total flow rate of 50 ml/min. The temperature was increased from 40 to 600 °C with a ramp of 5 °C/min, and was held constant at 600 °C for 30 min. For comparison, MoO_3 (99.95%, Alfa Aesar) and WO_3 (99.995%, Aldrich) were also commercially acquired.

2.1.4 Carburization and passivation

All carburization processes were performed in the TG-MS apparatus, in a flow of 20 ml/min of methane (or ethane), 70 ml/min of H_2 and 10 ml/min of argon. The temperature ramp was the same as used previously for the carburization of mono-metallic oxide precursors [16]. The synthesis of carbides was carried out at atmospheric pressure by heating from 40 to 450 °C at 5 °C/min and from 450 °C to the final, individually adapted, carburization temperature at 2 °C/min. All carbides were cooled to room temperature under flow of argon. During carburization, the mass spectrometer sampled the gas phase and recorded mass/charge ratios of 2-78. Before exposure of the carbides to the ambient, carbides were passivated isothermally at 40 °C with air diluted in argon. The concentration of O_2 was increased from 0.1% (4 hours) to 1% (6 hours) and to 16% (4 hours) in argon, with the total flow rates between 60 and 402 ml/min [16].

2.2 Catalyst characterization

2.2.1 Structure, elemental composition and texture

The bulk structure of the samples was characterized by powder X-ray diffraction (XRD) using a Bruker D8 instrument operating with Cu K_α radiation. The samples were measured in reflection geometry, and nickel metal powder (Matheson Coleman & Bell, 200 mesh) was used as a reference. Diffractograms were collected with scanning steps of 0.05° in 2θ over the angular range of 20-90°. The unit cell volume of the carbides was obtained by fitting the diffractograms peaks with Jade software.

The carbon content of the carbides was measured by combustion analysis in a CE-440 Elemental Analyzer. Molybdenum-to-tungsten ratios were determined by energy-dispersive X-ray spectroscopy (EDS) on a JEOL JSM-840A scanning electron microscope with a Kevex X-ray analyzer and IXRF software and digital imaging capability, operating at 15 kV.

BET surface areas were measured using a Micromeritics ASAP 2020 and N_2 at -196 ºC. Pore size distributions were determined by applying the BJH method to N_2 desorption isotherms. Prior to measuring the surface area, samples were degassed at a temperature of 350 °C for 4 h.

2.2.2 Surface and redox properties

The number of metal sites was measured by CO chemisorption; prior to CO chemisorption the previously passivated carbides were reduced in H_2 at 350 °C for 6 h and evacuated at 350 °C for

1 h, then cooled to 35 °C for CO chemisorption. Weakly adsorbed CO molecules were removed by degassing, and the CO adsorption isotherm was repeated. The difference between the first and the second isotherm was plotted and was extrapolated to zero pressure to calculate the amount of CO chemisorbed.

Temperature-programmed reduction (TPR) experiments were carried out in the TG-MS apparatus on about 11 mg of passivated carbides. A mixture of 80% H_2 in argon was streamed at a total flow rate of 100 ml/min. The temperature was held at 40 °C for 10 min and then increased from 40 to 700 °C at a ramp of 10 °C/min.

2.3 Catalytic tests: toluene conversion

Vapor phase conversion of toluene at elevated H_2 pressure in the temperature range from 193 to 400 °C served as test reaction. The reaction was conducted in flow in a 0.18 inch inner diameter stainless steel tubular reactor with Swagelok® connections. Varying amounts of passivated carbide powders (between 38 and 185 mg) were mixed with 200 to 300 mg SiC (Aldrich, 200-450 mesh) to avoid channeling and local heating and then loaded into the reactor. The reactor was placed into a 2 ft long electrical furnace, and the temperature was controlled using a thermocouple inside the reactor at the bottom of the catalyst bed. All samples were reduced at atmospheric pressure in a H_2 flow of 150 ml/min at a temperature of 350 °C for 1 h before the catalytic reaction. After reduction, the reactor was set to the desired temperature, and the back-pressure valve was set to achieve an absolute pressure of 21 bar. Toluene (99.5%, Mallinckrodt Chemicals) was introduced via a capillary at 0.02 ml liquid/min with an Eldex liquid feed pump. The capillary was inserted into the upper section of the reactor tube and touched the hot wall to avoid droplet formation. The toluene vapor was mixed with 150 ml/min STP H_2 (Ultra high purity, Airgas). The reactor effluent stream was analyzed every 30 min using an online HP 5890 GC equipped with a flame ionization detector and a 30 m, 0.32 mm GASPRO column. Transfer lines were heated to ensure that no condensation occurred between the reactor and the GC. The GC temperature program was, 5 min isothermal at 60 °C, then heating at 10 °C/min to a final temperature of 240 °C, which was held for 4 min.

Conversion of toluene was defined as the difference between moles of toluene in the feed and in the product divided by moles of toluene in the feed. Selectivity to compound *i* was calculated

as the moles of compound *i* times its carbon number divided by the moles of products times their carbon numbers. Turnover frequency (TOF) was calculated as the moles of toluene converted to methylcyclohexane divided by the number of accessible metal sites as determined by CO chemisorption.

3 Results

3.1 Synthesis of carbides

3.1.1 Calcination of freeze-dried precursors

Precursors containing FD-AHM, FD-APT and a mixture of FD-AHM and FD-APT with a molar fraction x_{Mo} = 0.5 were calcined in air at a final temperature of 600 °C. Assuming the compositions of the freeze-dried samples correspond to those of the starting materials, the theoretical weight losses to transform the freeze-dried precursors to their corresponding oxides are 18.47, 11.18 and 14.12%. The corresponding experimental values, which were derived from TG measurements during calcination (Figure S1), were 17.57, 11.81 and 14.58%, in good agreement with the predictions.

The final products after calcination with presumed stoichiometries MoO_3, WO_3 and $Mo_{0.5}W_{0.5}O_3$ exhibited the XRD patterns shown in Figure 1. The diffractograms of the monometallic oxides were similar to orthorhombic MoO_3(*oP*16) (ICDD: 00-005-0508) and monoclinic WO_3(*mP*32) (ICDD: 00-043-1035). The diffractogram of $Mo_{0.5}W_{0.5}O_3$ resembled that of WO_3, indicating partial substitution of tungsten by molybdenum in the WO_3 parent structure. Reflections of orthorhombic MoO_3 were absent in the mixed oxide samples.

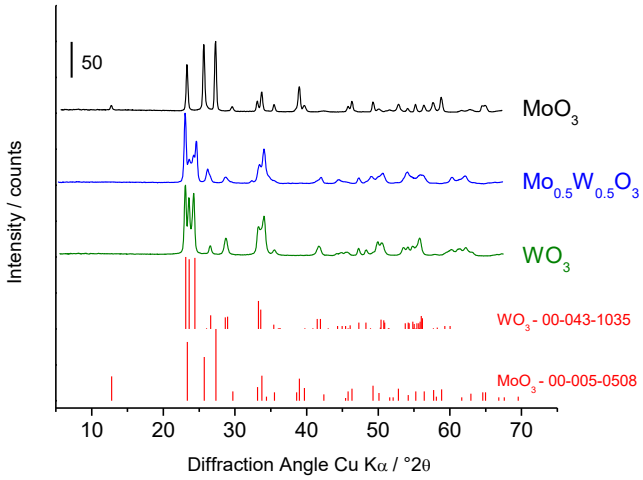

Figure 1: XRD patterns of calcined freeze-dried precursors.

3.1.2 Carburization of calcined freeze-dried materials

Weight changes and MS traces for the evolution of water (m/z=18) and CO (m/z=28) during carburization of the calcined freeze-dried materials are reported in Figure 2. The experimental weight losses for transformation of MoO_3, WO_3, and $Mo_{0.5}W_{0.5}O_3$ to Mo_2C, W_2C and MoWC were 29.6%, 18.64% and 21.5%, in good agreement with the corresponding theoretical weight losses of 29.18%, 18.12% and 22.35%. The TG-MS data also show that the first reduction step (well recognizable on the basis of the water formation in Figure 2b) of the mixed oxide $Mo_{0.5}W_{0.5}O_3$ occurred earlier by 75 and 60 ºC relative to the reduction of MoO_3 and WO_3, respectively. Notably, the WO_3 sample passed through a minimum in weight and after that, gained 1.28% in weight to give W_2C. In previously reported carburizations of commercial WO_3 samples, such a behavior has not been observed [16, 40]. The mass at the low point corresponds to a stoichiometry of $WO_{0.11}$, that is, the sample is largely composed of tungsten. WO_3 obtained by calcination of FD-APT was characterized by smaller particles (S_{BET}=7.6 m^2/g, d_p=110 nm) than commercial WO_3 (S_{BET}=1.5 m^2/g, d_p=524 nm). To check for further phase transformation, the temperature program was continued to 900 °C. After formation of the carbide at 650 °C, the weight increased in several steps, with weight gains of 0.7 and 2.1% relative to the weight at 650 °C. A weight gain of 3.1% would be expected for the transition of W_2C to WC. The weight then continued to increase gradually as the sample was heated past 770 °C, indicating carbon deposition on the surface (Figure 2).

(a)

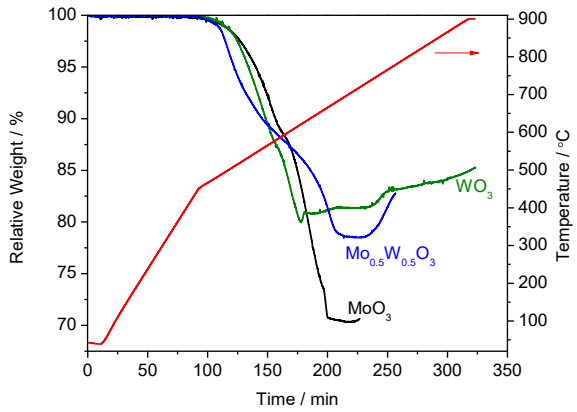

(b)

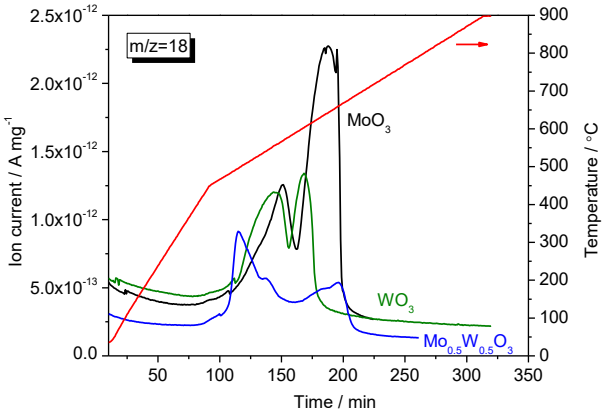

(c)

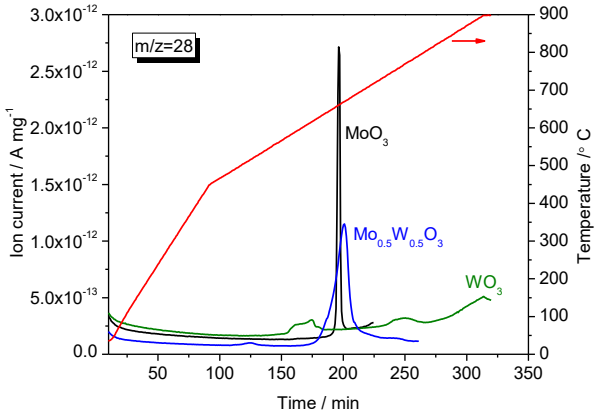

Figure 2: Carburization of calcined freeze-dried materials. Labels indicate starting materials. (a) Weight change, (b) water (m/z=18) formation, (c) CO (m/z=28) formation. Gas phase mixture 20%CH_4/70%H_2/10%Ar.

During carburization of all three oxides, two water peaks were observed as a result of reduction by H_2. A carbon monoxide peak appeared concomitantly with the second water peak (Figure 2).

The maxima of gas evolution for the three samples MoO_3, $Mo_{0.5}W_{0.5}O_3$ and WO_3 were located at 570, 497 and 556 °C (first H_2O peak), 645, 645 and 606 °C (second H_2O peak) and 660, 671 and 620 °C (CO peak). There was a second peak of CO at 772 °C during carburization of WO_3. The increase in the underlying m/z=28 signal for the WO_3 sample at higher temperature is associated with an increase in m/z=26 and 27 signals, indicating the formation of ethylene, which begins at about 700 °C.

3.1.3 Effect of precursor particle size on carburization

To assess the influence of the freeze-drying synthesis on the oxide properties, the carburization of MoO_3 prepared by calcination of FD-AHM was compared with that of commercial MoO_3. The results are presented in Figure 3. Both MoO_3 samples lost 28.55% of their initial weight, which is close to the theoretical value for Mo_2C formation of 29.18%. MoO_3 prepared from FD-AHM started to lose weight at significantly lower temperature than commercial MoO_3 (498 °C vs. 593 °C). Two reduction steps were clearly discernable for the MoO_3 obtained via freeze-drying synthesis, whereas commercial MoO_3 appeared to reduce in a single step. Presumably, the small particles of MoO_3 prepared by calcination of FD-AHM (S_{BET}=7 m^2/g, d_p=183 nm) as compared with the particle size of commercial MoO_3 (S_{BET}=0.3 m^2/g, d_p=4.3 µm), facilitated both reduction and carburization.

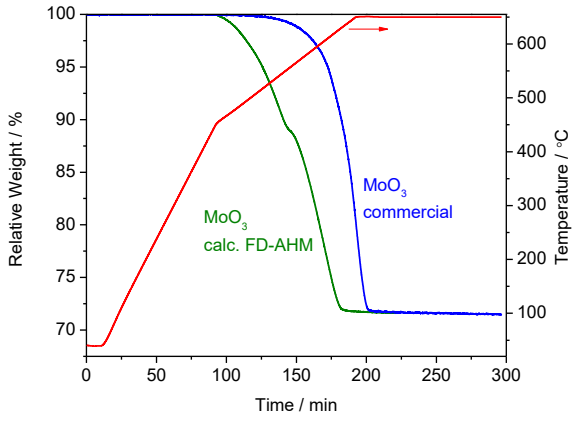

Figure 3: Thermogravimetric analysis of the carburization of commercial MoO_3 and MoO_3 prepared by calcination of FD-AHM. Gas phase mixture 10%C_2H_6/70%H_2/20%Ar.

3.1.4 Direct carburization of freeze-dried materials

To evaluate whether the calcination step can be omitted, the freeze-dried materials were directly carburized. The weight changes and the MS traces for water (m/z=18) and CO (m/z=28) formation are reported in Figure 4. The temperature was increased from 40 °C to the final carburization temperature, and heating was stopped before any surface carbon deposition (weight gain) was observed. Assuming the precursors have stoichiometries corresponding to mixtures of AHM and APT and the formed carbides have $Mo_{2-x}W_xC$ stoichiometry, the theoretical weight losses for the transformation of samples with x_{Mo} = 0, 0.25, 0.5, 0.75 and 1 are 27.27, 30.03, 33.32, 37.31 and 42.26%, respectively. The high atomic mass of tungsten implies that the percent weight loss becomes smaller as the tungsten content increases. The observed weight losses were 27.76, 29.73, 32.84, 36.21 and 41.19%, which can be considered in good agreement given the complexity of the precursor salts. In comparison to the oxides, the uncalcined precursors lost weight at lower temperatures and more gradually, and the gas product evolution was more complex because of counter ion decomposition. There were parallels as well; all tungsten-containing samples first lost weight with evolution of water, and then they gained weight, which coincided with CO evolution, but was not accompanied by water evolution (Figure 4). Based on the observed weight, tungsten-containing samples had a stoichiometry of $Me_2O_{\sim 0.5}$ (Me=Mo+W) when they reached their minimum in weight. The precursor with x_{Mo}=0.75 reached the minimum at 100 ºC lower temperatures than the other tungsten-containing samples (at 550 °C and with a broad water peak). After passing through the minimum, the samples with x_{Mo}=0, 0.25, 0.5 and 0.75, gained 1.22, 1.3, 1.27 and 0.33% in weight, respectively. During carburization of FD-APT, a continuous weight gain was observed even after termination of CO formation (not shown), which is ascribed to the deposition of carbon on the surface. In order to avoid surface contamination with carbon, the final carburization temperature for FD-APT did not exceed 650 °C. For the molybdenum-rich samples, CO formation overlapped with water formation. FD-AHM gave a large CO peak, which was eight times larger than the size of the CO peaks during carburization of FD-APT. Accounting for the different molecular weights, less than a factor of 2 would be expected if the step had the same relevance in the carburization process of these two materials.

(a)

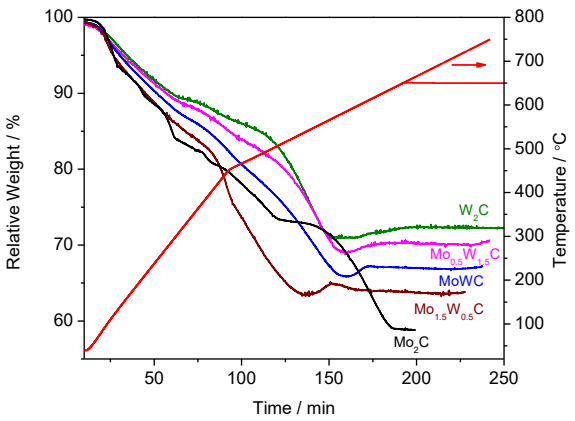

(b)

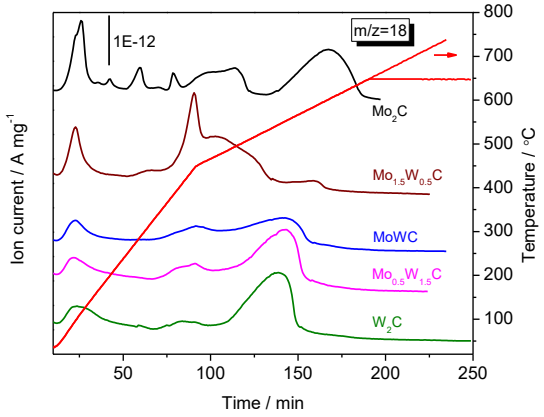

(c)

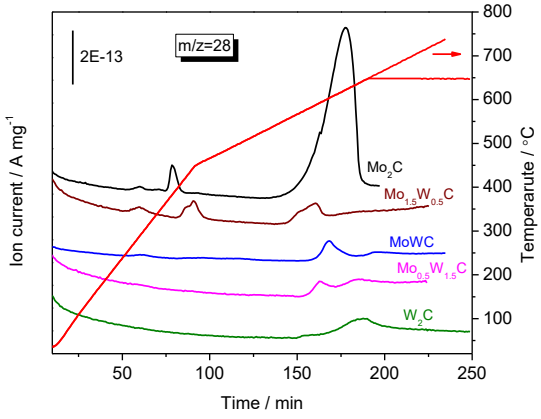

Figure 4: Direct carburization of FD precursors. Labels indicate the final carbides. The isothermal process was for temperature-programmed carburization of FD-APT. (a) Weight change, (b) water (m/z=18) formation, (c) CO (m/z=28) formation. Gas phase mixture 20%CH_4/70%H_2/10%Ar.

The carbides from the syntheses reported in Figure 4 were used for XRD measurements. For characterization and activity measurements, a set of carbide samples was prepared at a final temperature of 650 °C, since there was no further weight change between 650 and 750 °C. Samples were held at 650 °C until CO formation stopped and no weight change was observed with TG-MS.

3.1.5 Passivation of carbide surface

Metal carbides are pyrophoric and need to be passivated before coming in contact with the ambient, typically by creating a thin oxide skin on the surface. Passivation was conducted starting with a low concentration of 0.1% O_2 and then slowly increasing the concentration; this protocol allows for the recovery of more metallic sites during regeneration [16]. The weight gain resulting from oxygen uptake was in the range of a few percent for all Mo-W carbides synthesized at 650 ºC, as reported in Table 1. Considering the different molecular weights of Mo_2C and W_2C (204 and 380 g mol^{-1}), the oxygen-to-metal stoichiometry after passivation was comparable for the two monometallic carbides. The bimetallic carbides were characterized by higher oxygen uptakes, with the highest value observed for MoWC (2.55%). A sample with x_{Mo}=0.5, and prepared up to 590 ºC, when it was nearly metallic, (TG data in Figure 4) also reacted with O_2 at room temperature, resulting in an oxygen uptake of 2.8%.

3.2 Characterization of carbide properties

3.2.1 Structure, elemental composition and texture

The bulk structure of the metal carbides was analyzed by XRD. The diffractograms of carbides that were prepared by carburization of oxides are reported in Figure 5. Molybdenum carbide was hexagonal (ICDD: 00-035-0787) as reported in Figure 5.3. Tungsten carbide prepared at a final temperature of 750 °C consisted of a single phase with hexagonal structure (ICDD: 00-035-0776) (Figure 5.4), whereas tungsten carbide that was prepared at 900 °C contained two hexagonal phases, W_2C(*hP*3) (ICDD: 00-035-0776) and WC(*hP*2) (ICDD: 00-051-0939) (Figure 5.6). Two MoWC samples that were prepared at 700 °C (Figure 5.8) and 800 °C (Figure 5.9) consisted of two phases similar to hexagonal W_2C(*hP*3) (ICDD: 00-035-0776) and cubic WC(*cF*8) (ICDD: 00-020-1316).

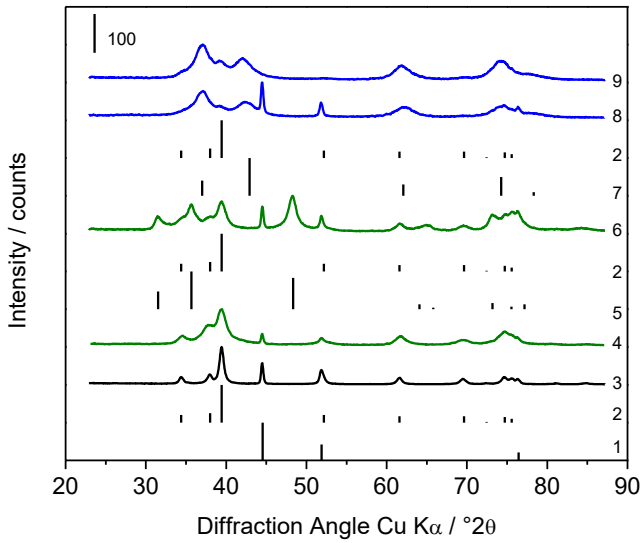

Figure 5: XRD patterns for Mo-W carbides prepared by carburization of oxides. From bottom to top: (1) Ni (ICDD:00-004-0850), (2) Mo_2C (ICDD:00-035-0787), (3) Mo_2C prepared from MoO_3 at 720 °C, (4) W_2C prepared from WO_3 at 750 °C, (5) WC (ICDD: 00-051-0939), (6) tungsten carbide prepared from WO_3 at 900 °C, (7) WC (ICDD: 00-020-1316), (8) MoWC prepared from $Mo_{0.5}W_{0.5}O_3$ at 700 °C, (9) MoWC prepared from $Mo_{0.5}W_{0.5}O_3$ at 800 °C.

The diffractograms of the metal carbides that were prepared by direct carburization of freeze-dried precursors are reported in Figure 6a. Molybdenum carbide that was synthesized by direct carburization of FD-AHM consisted of a single phase with the hexagonal structure of Mo_2C(*hP*3) (ICDD: 00-035-0787), and tungsten-containing carbides consisted of a single phase with a structure similar to hexagonal W_2C(*hP*3) (ICDD: 00-035-0776). These two structures are similar to each other with nearly identical unit cell volumes of 37.21 $Å^3$ (Mo_2C) and 36.78 $Å^3$ (W_2C). According to Vegard's Law, a gradual contraction would thus be expected with increasing tungsten content. This trend was less pronounced than anticipated (Table 1) as will be discussed later.

To better understand the carburization process and the associated phase transitions, additional XRD patterns were recorded that are shown in Figure 6b. Direct carburization of the FD precursor with x_{Mo} = 0.5 to a temperature of 590 °C (where the minimum weight was reached) resulted in the formation of a near-metallic phase of MoW, as indicated by a diffractogram similar to that of metallic tungsten W(*cI*2) (ICDD: 00-004-0806). The carburization of FD-APT at 870 °C resulted in the formation of single-phase hexagonal WC(*hP*2) (ICDD: 00-025-1047).

(a)

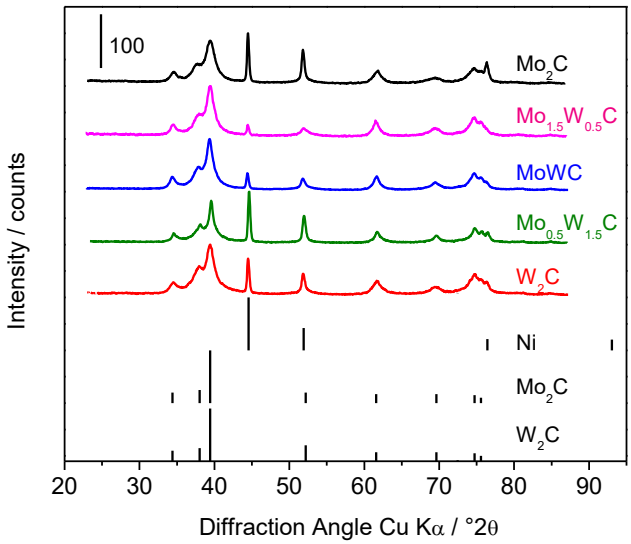

(b)

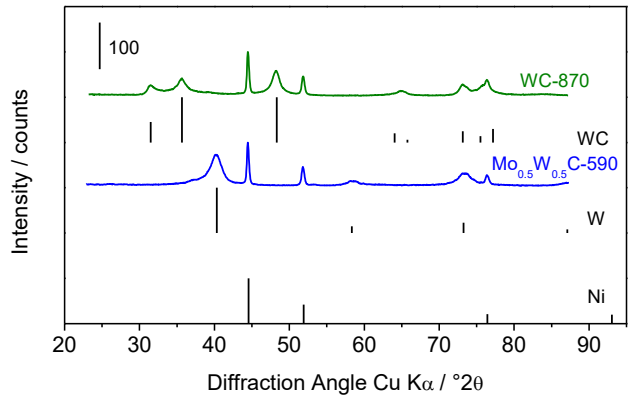

Figure 6: XRD patterns of carbides prepared by direct carburization of freeze-dried precursors in comparison with reference stick patterns. Ni used as the internal standard. (a) Carbides from syntheses shown in Figure 4. (b) FD sample with $x_{Mo}=x_{W}=0.5$ carburized at 590 °C, WC prepared by carburization of FD-APT at 870 °C. References: Ni (ICDD: 00-004-0850), Mo_2C (ICDD: 00-035-0787) and W_2C (ICDD: 00-035-0776), W (ICDD: 00-004-0806), WC (00-025-1047.

Metal ratios, carbon contents and textural properties of the carbides prepared by direct carburization of freeze-dried precursors are summarized in Table 1. The metal ratios were determined from EDX measurements recorded at multiple locations on different particles, and an average is reported for each carbide. The EDX data in Table 1 demonstrate that the mixed metal carbides are homogenous in composition at the micron level, and the final metal ratios are very

close to the intended values. The carbon content was close to the theoretical values based on an assumed metal-to-carbon ratio of 2 (stoichiometry $Mo_{2-x}W_xC$, $0 < x < 2$). The pore volume and pore diameter of mono-metallic carbides were higher than those of mixed metal carbides. This behavior is consistent with the higher amount of oxygen uptake of mixed metal carbides, as oxygen adsorption causes a decrease in pore volume of metal carbides [16]. W_2C had the lowest CO uptake (15.2 μmol/g) and by increasing the molybdenum content, the amount of CO uptake was increased to the maximum value for Mo_2C (26.6 μmol/g). The N_2 physisorption isotherms were type IV with a pore size distribution in the meso-porosity range.

Table 1: Characterization data for Mo-W carbides prepared by direct carburization of freeze-dried precursors

Sample	$x_{Mo}=n_{Mo}/(n_{Mo}+n_W)$		Carbon content (%wt)		Cell volume ($Å^3$) [c]	Weight gain during passivation (%wt)[d]	SA_{BET} (m^2/g)[e]	BJH pore diameter (Å)[e]	BJH volume (cm^3/g)[e]	CO uptake (μmol/g)
	Loaded	Measured by EDX [a]	Theoretical[b]	Measured						
Mo_2C	1.00	1.00	5.88	5.79±0.18	37.43	1.76	19.1	84.0	0.041	26.6
$Mo_{1.5}W_{0.5}C$	0.75	0.79	4.85	4.61±0.20	37.42	2.38	21.8	67.4	0.028	24.7
MoWC	0.50	0.54±0.03	4.11	4.03±0.13	37.51	2.55	16.0	53.2	0.015	20.9
$Mo_{0.5}W_{1.5}C$	0.25	0.26±0.06	3.57	3.28±0.06	37.00	2.26	13.8	54.6	0.023	21.4
W_2C	0.00	0.00	3.16	3.10±0.17	37.39	1.08	20.5	72.9	0.046	15.2

[a] Measured on different particles, average values with standard deviations were reported. [b] based on assumption of Me/C=2.
[c] Samples from Fig. 4. Volume calculated based on $V_{cell}=a\times b\times c\times \sin(60°)$, Mo_2C (ICCD=00-035-0787) has $V_{cell}=37.21$ $Å^3$ and W_2C (ICCD=00-035-0776) has $V_{cell}=36.78$ $Å^3$. [d] Basis was freshly prepared carbide before exposure to ambient. [e] Measured after passivation.

3.2.2 Reduction of passivated carbides

To identify an appropriate temperature for removal of the passivation layer, the samples were heated in H_2 at atmospheric pressure. MS analyses of the volatile products of these TPR experiments are shown in Figure 7. The main gas phase products were water (m/z=18) and methane (m/z=15). For all carbides, water started to form in the temperature range of 100 to 150 °C and continued to about 350 to 400 °C. The MS traces exhibited two overlapping peaks. The low temperature peak dominated for the molybdenum-rich samples, while the high-temperature gradually increased with tungsten content.

(a)

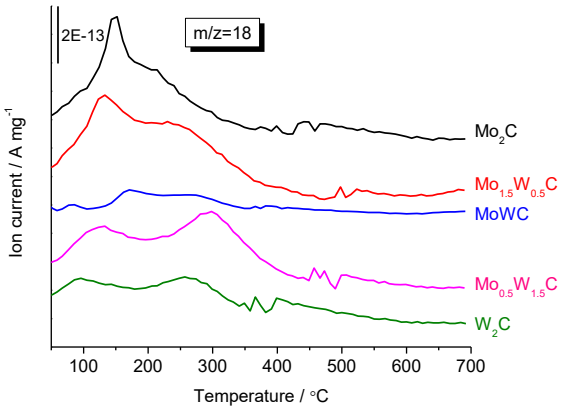

(b)

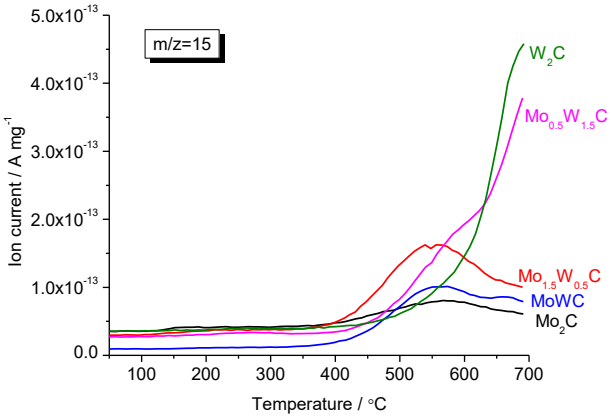

Figure 7: MS data for temperature-programmed reduction of passivated carbides synthesized at a final carburization temperature of 650. Water (a) and methane (b) formation. Gas phase mixture 80% H_2 in Ar.

Methane evolution started at a temperature of around 400 °C for all carbides. For the molybdenum-rich samples Mo_2C, $Mo_{1.5}W_{0.5}C$ and MoWC, methane evolution was transient with a maximum at 550 °C. The tungsten-rich samples $Mo_{0.5}W_{1.5}C$ were characterized by a rapidly increasing methane formation rate above 600 °C.

Based on the TPR data, all passivated carbides were reduced at 350 °C prior to the catalytic reactions. At this temperature, oxygen can be removed from the surface without damaging the underlying carbidic surface.

3.3 Catalytic activity

Conversion of toluene was used to test the catalytic activity of the carbides at different temperatures between 193 and 275 °C and at 400 °C. For all carbides, the only product formed below 275 °C was methylcyclohexane (MCH). The reaction rate was assumed to be zero order with respect to toluene [3], and an Arrhenius plot was generated to determine the activation energies for ring hydrogenation of toluene to MCH (Figure 8). The temperature was first increased from 193 to 275 ºC in steps of 10 ºC, and then decreased, to be able to detect any deactivation, which, however, was absent. At each temperature, rates were averaged over 1.5 hours.

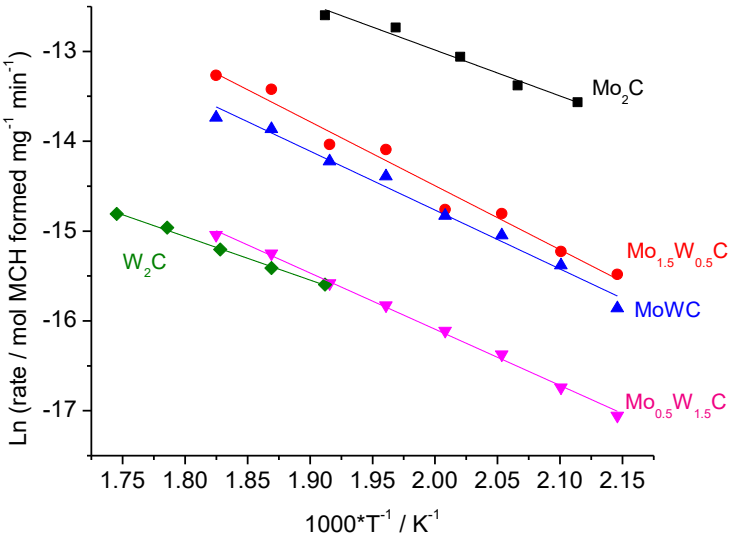

Figure 8: Arrhenius plot for hydrogenation of toluene to methylcyclohexane on Mo-W carbides. Reaction conditions: P=21 bar and temperature range of 193 to 275 °C.

The activation energies for hydrogenation of toluene to MCH on mono-metallic carbides of Mo_2C and W_2C were comparable within the uncertainty of the measurement (≈ 42 kJ/mol). However, on mixed metal carbides, higher activation energies between 52.0 and 59.2 kJ/mol were observed (Table 2).

Table 2: Activation energies for hydrogenation of toluene to methylcyclohexane on Mo-W carbides. Temperatures in the range of 193 to 275 °C and total pressure of 21 bar.

Sample	E_a (kJ/mol)
Mo_2C	42
$Mo_{1.5}W_{0.5}C$	59.2
MoWC	54.5
$Mo_{0.5}W_{1.5}C$	52.0±0.9*
W_2C	40.3±2.4*

*Measured two times, from two different batches. Average values with standard deviations are reported.

Turnover frequencies (TOF) for ring hydrogenation of toluene to MCH on Mo-W carbides at 250 °C and 21 bar pressure are reported in Figure 9. The results indicated that Mo_2C had the highest hydrogenation activity per active site (2.1 s^{-1}) and that the hydrogenation activity decreased with increasing tungsten content in the mixed metal carbides, reaching the lowest value of 0.15 s^{-1} for W_2C.

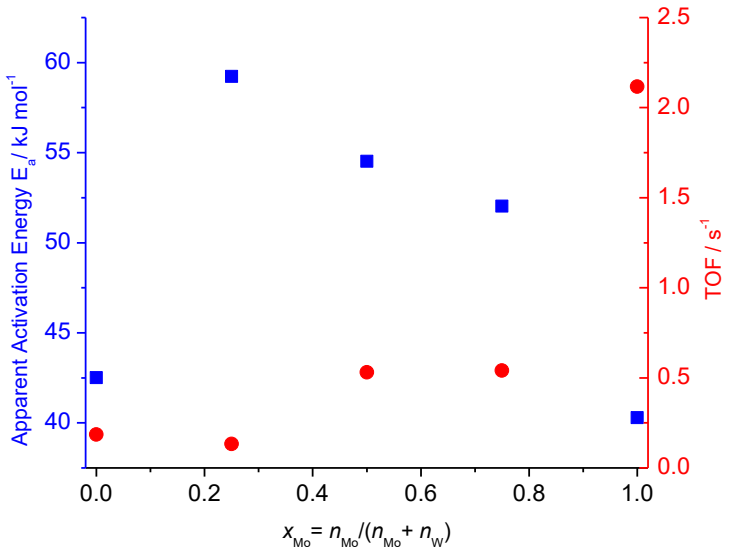

Figure 9: Apparent activation energies and TOFs for hydrogenation of toluene to methylcyclohexane at 250 °C and 21 bar H_2 pressure. Activation energies values are from Table 2.

The carbides were also tested at 400 °C to explore their selectivity for reactions other than ring hydrogenation. At this temperature, all carbides deactivated over a period of several hours, as reported in Figure 10. Over a period of 24 h, Mo_2C showed the highest loss of about 52% relative to the initial activity, whereas $Mo_{0.5}W_{1.5}C$ showed the lowest loss about 17% relative to the initial activity. However, the turnover number of Mo_2C after 24 h was 56 mmol of toluene converted/g catalyst and thus much higher than that of $Mo_{0.5}W_{1.5}C$, which was only 9 mmol of toluene converted/g catalyst.

The selectivity after 24 h on stream at 400 °C (when steady state was reached, Figure 10) at comparable conversions (≈44%) is reported in Table 3 for the entire series of Mo-W carbides. At high conversions, that is, initially, hydrogenolysis products (C_1-C_6) were predominant. As deactivation progressed, products such as MCH, ethylcyclopentane (ECP), benzene and xylene were formed. Selectivity to ECP was less than 2% for all carbides. Tungsten-rich carbides showed lower hydrogenolysis activity and formed more benzene than molybdenum-rich carbides.

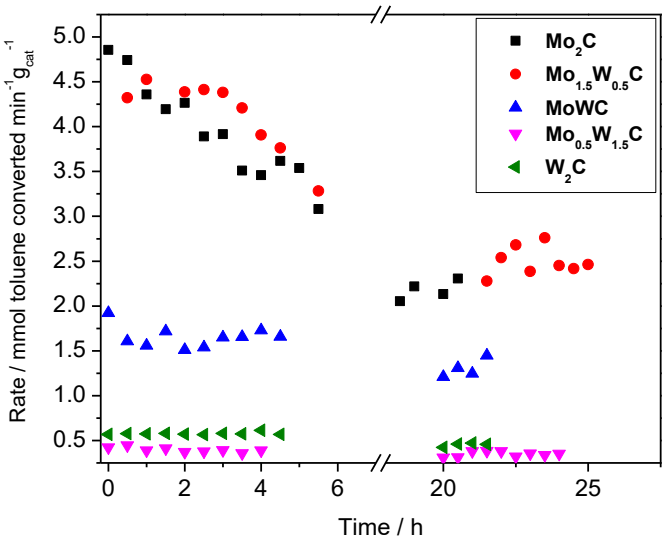

Figure 10: Stability of Mo-W carbides series during toluene hydrogenation at a temperature of 400 °C, a molar ratio of H_2/toluene = 33 and a total pressure of 21 bar. W/F ranged from 0.04 to 0.20 h. Corresponding selectivities are reported in Table 3.

Table 3: Product selectivity for toluene conversion on Mo-W carbides at 400 ºC and 21 bar pressure.

Sample	W/F (h)	Conv. (%)	Selectivity (C-mol%)[1]				
			C_1-C_6	MCH	Benzene	ECP	Xylene
Mo_2C	0.04	44.6	63.8	18.3	10.9	1.1	6.0
$Mo_{1.5}W_{0.5}C$	0.04	54.2	69.7	8.6	16.3	0.7	4.7
MoWC	0.06	44.1	55.4	21.1	18.1	1.1	4.2
MoWC	0.02	15.6	34.7	40.4	15.7	1.6	7.6
$Mo_{0.5}W_{1.5}C$	0.20	41.9	55.8	19.6	18.9	1.0	4.7
W_2C	0.18	44.5	58.1	19.4	17.6	1.1	3.9

[1] Selectivity is average of 2-4 hours of data after steady state has been reached (after 18 to 22 hours of reaction).

4 Discussion

4.1 Synthesis of metal carbides

4.1.1 Reduction and carbide formation

Carburization of an oxidic precursor in a gas mixture of H_2 and a hydrocarbon (methane in this work) is often a diffusion-limited process that occurs in several steps involving reduction and carbon incorporation. Oxygen species diffuse out, and carbon species migrate into the lattice. H_2 and the hydrocarbon can both serve as reducing agents, but H_2 is typically activated at lower temperature and on a less reduced surface, leading to a first reduction step. The carbon in methane can be oxidized to carbon or carbon oxides while the hydrogen in methane can be reduced to H_2 or react to water, depending on the availability of residual oxygen. Once the hydrocarbon can be activated, further reduction to the metal and carbide formation are competing processes. A rate of reduction exceeding that of carbon incorporation may lead to a metallic bulk and potential sintering [41]. Gas phase composition, temperature program, and precursor determine the relative rates [42].

The flash-freezing and freeze-drying process produced small particles, which were to some extent retained after calcination. The resulting short diffusion paths led to earlier reduction of MoO_3 by H_2, and molybdenum carbide formation was complete at about 50 °C lower temperature than for coarse crystalline MoO_3 (Figure 3). The synthesis method thus has great potential to achieve high surface area carbides.

However, when tungsten was present, some of the samples were deeply reduced before methane was activated. For FD-derived WO_3, the minimum weight suggests a near-metallic state, which is ascribed to the smaller particle size of this material in comparison to commercial WO_3. To characterize the extent of reduction in FD-precursor-derived samples, the state of a sample with x_{Mo}=0.5 at the weight minimum (590 °C) was investigated. At this temperature, the stoichiometry of the sample was $MoWO_{0.52}$, and the diffractogram was similar to that of metallic tungsten (Figure 6b). This near-metallic intermediate makes it more likely that sintering could occur prior to carbide formation.

Several general trends can be explained in light of the considerations above on the carburization process. The TG profiles of the tungsten-containing precursors were closer to those of FD-APT than to that of FD-AHM (Figure 4). Uncalcined precursors were reduced earlier than

the more stable oxides; the freeze-dried precursors are amorphous, may have smaller particles than the oxides, and thus reduced diffusion lengths. Mixed oxides and mixed uncalcined precursors were reduced at lower temperatures than the corresponding monometallic materials. Presumably, lattice distortion or defects in the mixed materials increase oxygen mobility (diffusivity) allowing the lower temperature for bulk reduction [43,44].

For the FD-derived oxides, CO production starts at lower temperatures for tungsten-rich samples than for the pure molybdenum samples (at bulk compositions of $WO_{1.24}$, $Mo_{0.5}W_{0.5}O_{1.42}$, and $MoO_{0.88}$ based on TG data), whereas for the FD precursors, CO production occurs first in the molybdenum-rich sample. The more well-defined profiles of the oxide samples provide some explanations for the observed trends. Reduction of the Mo-W mixed oxide is a drawn-out process, and the material is not reduced enough to activate methane until about 620 °C. Large particle size, or a less reactive surface could be the origin of this behavior. The molybdenum oxide sample shows a late first and then an extremely rapid second reduction step (TG slope) and a spike in CO production at about 650 °C. A tentative interpretation is that the high surface area of the MoO_2 intermediate allows such a rapid reduction that the water product leaving the surface blocks the methane from the surface. Only when the water peak starts to decrease can methane approach the surface and rapidly carburize the molybdenum while reacting with residual oxygen to CO.

4.1.2 Evolution of carbide crystalline phases

Carburization of precursors containing only molybdenum (FD-AHM and FD-derived MoO_3) resulted in formation of hexagonal Mo_2C(*hP*3), consistent with the structure that is typically obtained upon carburization of commercial MoO_3 in a H_2/hydrocarbon atmosphere [16]. Hence, there is no significant influence of the precursor on structure. Interestingly, four of the five samples in Table 1 have roughly the same unit cell volumes, implying that the series does not obey Vegard's law for solid solutions. The materials were produced at relatively mild final temperatures between 650 and 750 °C, and their diffractograms in Figure 6a show very broad reflections, consistent with small, disordered particles. This disorder may be responsible for the lack of adherence to Vegard's law.

The XRD patterns in Figure 6 and TG data demonstrate that direct carburization of FD-APT resulted in the formation of hexagonal W_2C(*hP*3) at 680 °C, and subsequent transformation into

hexagonal WC(*hP*2) by 870 °C. This sequence is consistent with literature showing the synthesis of W_2C in 10% ethane is followed by a transition to WC [40]. This phase transformation was slower for carburization of FD-derived WO_3. At 750 °C it formed W_2C with a hexagonal structure (Figure 5.4), but this structure was only partially converted to WC(*hP*2) by 900 °C (Figure 5.6). The very rapid and more complete reduction of FD-APT before methane is activated – water evolution is finished 25 °C earlier than for FD-derived WO_3 – produces a less stable (perhaps higher surface area) W_2C, which is more easily converted to WC.

Equally, a single phase mixed metal carbide could not be prepared by carburization of $Mo_{0.5}W_{0.5}O_3$. Both at 700 and 800 °C, the mixed oxide transformed into a mixture of cubic WC and hexagonal W_2C or Mo_2C (Figure 5.8 and 9).

Formation of tungsten carbide WC with the cubic structure is noteworthy. Previously published routes to cubic WC_{1-x} or MoC_{1-x} include carburization of cubic structure tungsten or molybdenum nitrides resulting in a topotactic transformation to carbides [45], adding small amounts of nickel or platinum to the oxide precursor to promote H_2 activation during carburization [46], and pre-reduction of MoO_3 [47]. The latter two routes can be seen as two methods to achieve reduction prior to carbon incorporation, which results in structural rearrangement [48]. As the TG data in Figure 2 clearly show, $Mo_{0.5}W_{0.5}O_3$ is initially more rapidly reduced than the monometallic oxides. Attempts to obtain a single-phase carbide by varying the heating rate (2, 5 or 10 °C/min) during carburization of $Mo_{0.5}W_{0.5}O_3$ were not successful. Possible solutions to obtain the single-phase cubic carbide from $Mo_{0.5}W_{0.5}O_3$ could be via carburization of a mixed metal nitride with cubic structure [31], or via carburization of an oxyhydride in high concentration of ethane [49].

In conclusion, carburizing precursors obtained via flash-freezing and freeze-drying without a calcination step is a convenient route to single phase pure and mixed metal carbides with Me_2C stoichiometry and hcp structure (Figure 5 and Figure 6a).

4.2 Properties of Mo-W carbide series

4.2.1 Composition, texture and surface properties

As expected, the compositions of the carbides obtained via direct carburization reflected those of the starting solutions (Table 1). Moreover, standard deviations of EDX measurements were small, demonstrating good uniformity of the composition. The carbides were only slightly carbon-

deficient, indicating that the near-metallic state of the tungsten-containing samples does not inhibit carbon incorporation. The surface areas of the pure carbides were on the lower end of the range reported for the passivated state in the literature [6,12,16,19,40]. Here, some optimization may be possible by using ethane instead of methane [50] to exploit the more facile first reduction step and the lower carburization temperatures that are unique to these precursors. The CO uptakes were within the range of reported values for Mo_2C and W_2C [5,7,16]. The main advantages of the synthesis method are the adjustable and uniform composition. The rather small variations in surface area and the monotonic trend in the CO uptake demonstrate the reliability and consistency of the synthesis method.

4.2.2 Reduction of passivated carbides

When removing the passivation layer, the optimal temperature is one that removes all oxygen and does not remove carbon. Temperature-programmed reduction experiments indicated that 350 °C is a good compromise that works for the entire series of mixed Mo-W carbides. For all samples, two peaks of water were observed, which can arise from the presence of two different sites or removal of oxygen from surface and subsurface locations [51]. The onset of methane formation was earlier for molybdenum-rich samples, but the peak was small, indicating that the surfaces of molybdenum-rich carbides can be preserved better in the presence of hydrogen than those of tungsten-rich carbides. W_2C and the $Mo_{0.5}W_{1.5}C$ samples lose carbon at an accelerated rate at over 600 ºC, suggesting a maximum operating temperature for these samples in a strongly reduction atmosphere. Moreover, when reduction was performed at 21 bar pressure (similar to reaction pressure, not shown), MoWC started to lose carbon in the form of methane at about 300 ºC, implying that above a certain temperature, surface stoichiometry of these mixed carbides will be a function of reaction conditions.

4.3 Catalytic performance

4.3.1 Toluene ring hydrogenation to methylcyclohexane on mixed Mo-W carbides at 250 ºC

All carbides prepared by direct carburization were active for hydrogenation of toluene to MCH at 21 bar H_2 and 250 °C. The specific rate for MCH formation decreased with increasing tungsten content in the carbides (Figure 8). This trend is in agreement with the decreasing number of noble metal-like sites titrated by CO, upon increasing the tungsten content in Mo-W carbides (Table 1).

However, the rates were more strongly affected by tungsten addition than the number of (single atom) sites, as the resulting TOFs demonstrate (Figure 9). Mo_2C was characterized by a higher TOF than W_2C, but the TOFs declined rapidly with tungsten incorporation. Such a trend would be expected for a reaction that requires an ensemble site, and toluene hydrogenation is known to be structure-sensitive (on noble metals) [52,53]. The surface is thus clearly altered by the presence of tungsten and is not molybdenum-enriched as observed for samples prepared at high temperatures [21].

TOFs ranged from 0.2 s^{-1} for W_2C to 2.1 s^{-1} for Mo_2C. Notwithstanding the higher reaction temperature of 250 °C, they were not significantly higher than previously measured TOFs of 1.8 s^{-1} for Mo_2C at 150 °C and 0.2 for W_2C at 200 °C [16]. This result is ascribed to a non-optimal temperature during reduction after passivation; to keep the temperature the same for the entire series, 350 °C was chosen as a compromise instead of the previously used 300 °C for Mo_2C and 400 °C for W_2C.

The activation energies for ring hydrogenation of toluene that were observed with the carbide series (Table 2) were in the range of 40 to 59 kJ/mol, which compares well with values reported for noble metals: 40-50 kJ/mol on Pt/ZSM-22 [54] and 29-55 kJ/mol on supported Pd [55]. An activation energy of 58.1 kJ/mol was reported for hydrogenation of toluene to MCH on molybdenum carbide; which is higher than the value found in this work (42 kJ/mol). This difference is explainable, because the molybdenum carbide used by Frauwallner et al. was of cubic structure and contained an oxide impurity [3]. Activation energies for the ring hydrogenation of toluene (which is a structure sensitive reaction) were higher for mixed-metal carbides than for mono-metallic carbides (Table 2), implying differences in the nature of the active sites. Dehydrogenation of cyclohexane on Mo-W carbides showed the same trend, similar activation energies for mono-metallic carbides, and higher activation energies for mixed metal carbide [39].

4.3.2 Reaction of toluene on mixed Mo-W carbides at 400 °C

Initially, at 400 °C and high conversions, light products (C_1-C_6) were predominant, consistent with hydrogenolysis following as a secondary reaction after ring hydrogenation. This interpretation is corroborated by the selectivity of MoWC at low conversion, which favors methylcyclohexane over C1-C6 alkanes. The cause for deactivation could be surface restructuring,

removal of residual oxygen, carbon depletion, or carbon deposition. Restructuring at high temperature would probably increase the number of ensemble sites, which should promote toluene ring hydrogenation. Oxygen removal should also be favorable for hydrogenation, as it should remove acid sites and enhance the metallic character. Given that Mo_2C and W_2C become more active at low temperatures after operation at higher temperatures [16], carbon deposition, which makes the surface inert and less active for hydrogenolysis [39], can also be excluded as a cause. Carbon depletion, which has to be considered at the applied H_2 pressure, would slightly lower the hydrogen affinity and considerably strengthen the carbon affinity of the surface, and appears to be the best explanation for the decreasing activity for toluene ring hydrogenation. The steady state composition of the Mo-W carbides is thus likely different from the starting composition and a function of conditions (*i.e.*, hydrogen and carbon chemical potential).

As activity declined with time on stream, MCH, benzene, xylene and ECP were observed (Table 3). Both disproportionation and ring contraction imply acid sites. The presence of different sites such as metallic, acidic or dual sites has been reported for oxycarbides and nitrides [4], and the origin of acidity (Brønsted acid sites) has been attributed to the presence of residual oxygen on the surface of metal carbides [6-9]. On all of the Mo-W carbides in this work, the selectivity to ECP was less than 2% (Table 3). Ring contraction of six-membered rings to five-membered rings needs strong Brønsted acid sites [56], and only a low number of metallic sites and a high number of Brønsted sites will favor ring contraction products [57]. The concentration of acid sites on molybdenum carbide is too low to catalyze ring contraction [58], and apparently, addition of tungsten does not result in a significant increase in acidity.

Benzene and xylene can be attributed to disproportionation of toluene. However, since more benzene than xylene was formed, dealkylation has to be inferred (Table 3). As shown by TPR data in Figure 7, creation of carbon vacancies is possible under reaction conditions. The carbon vacancy sites can serve as active sites for dealkylation, in a similar fashion as direct desulfurization by sulfur vacancies in sulfides [59] or deoxygenation by oxygen vacancies in oxide catalysts [60]. Consistent with this view, the affinity of the surface for carbon is known to increase dramatically during the transition from stoichiometric carbide to pure metal [11]. Moreover, Mo_2C, which is most resilient towards carbon loss (Figure 7), produces the least amount of benzene.

Overall, hydrogenation and hydrogenolysis products were predominant (Table 3), implying that in Mo-W carbides metal sites prevail over acid sites. In contrast, niobium-rich mixed carbide Mo-Nb carbides (with NbC structure) [18] formed more acid-catalyzed products, specifically ring contraction products. This gradation is in line with higher oxophilicity of niobium in comparison with tungsten, which is expected to lead to increased oxygen retention and a higher number of acid sites, and with lower activity of niobium carbide for hydrogenation and hydrogenolysis.

5 Conclusions

A series of single phase Mo-W carbides with Me_2C stoichiometry and hexagonal structure was successfully synthesized by direct carburization of precursors with intimately mixed metals. The precursors were obtained via flash-freezing of aqueous solutions of tungsten and molybdenum salts and subsequent freeze-drying. The fine precursor particles were reduced more rapidly than coarse crystalline oxides during the carburization process, opening avenues to lower carburization temperatures and possibly higher surface areas. However, all tungsten-containing materials passed through a near-metallic state; and to avoid this deep reduction and possibly associated sintering, methane may have to be replaced with a more reactive hydrocarbon.

All carbides were catalytically active for ring hydrogenation of toluene at high H_2 pressure and temperatures of 193 to 275 °C, with activation energies ranging between 40 and 60 kJ/mol and hence comparable with those reported for noble metals. Mo_2C had the highest hydrogenation activity per site (with number of sites probed by CO). The decline in turnover frequency with increasing tungsten content was stronger than anticipated by interpolation between the two monometallic carbides, suggesting an additional effect such as breakup of ensemble sites.

During operation at 400 °C and 21 bar, all carbides deactivated before reaching steady at about 24 h on stream. The highest loss relative to initial rates was seen for Mo_2C (53%) and the lowest for $Mo_{0.5}W_{1.5}C$ (17%); while Mo_2C reached a much higher turnover number than $Mo_{0.5}W_{1.5}C$. Selectivity was a function of conversion, and, at high conversions prior to deactivation, light gases (C_1-C_6) dominated because of hydrogenolysis as a secondary reaction after ring hydrogenation. At steady state, alkanes, methylcyclohexane, benzene, xylene and traces of ethylcyclopentane were formed indicated metallic (hydrogenation and hydrogenolysis), Brønsted acid (disproportionation)

and vacancy sites (dealkylation leading to benzene excess over xylene). The presence of tungsten promoted carbon vacancy formation and dealkylation.

Acknowledgement

Acknowledgment is made to the Donors of the American Chemical Society Petroleum Research Fund for support (or partial support) of this research under PRF#51448-ND5) and the U.S. Department of Energy under Grant No. DE-SC0004600. This work was, in part, supported by NSF award 0923247 (thermal analysis equipment as part of a major research instrumentation grant. The author thanks Lance L. Lobban for providing the test reactor and Alana Denning for her assistance with EDX measurements.

References

[1] R.B. Levy, M. Boudart, Platinum-Like Behavior of Tungsten Carbide in Surface Catalysis, Science, 181 (1973) 547-549.
[2] J.R. Kitchin, J.K. Nørskov, M.A. Barteau, J.G. Chen, Trends in the chemical properties of early transition metal carbide surfaces: A density functional study, Catalysis Today, 105 (2005) 66-73.
[3] M.-L. Frauwallner, F. López-Linares, J. Lara-Romero, C.E. Scott, V. Ali, E. Hernández, P. Pereira-Almao, Toluene hydrogenation at low temperature using a molybdenum carbide catalyst, Applied Catalysis A: General, 394 (2011) 62-70.
[4] J.-S. Choi, G. Bugli, G. Djéga-Mariadassou, Influence of the Degree of Carburization on the Density of Sites and Hydrogenating Activity of Molybdenum Carbides, Journal of Catalysis, 193 (2000) 238-247.
[5] G.S. Ranhotra, A.T. Bell, J.A. Reimer, Catalysis over molybdenum carbides and nitrides, Journal of Catalysis, 108 (1987) 40-49.
[6] F.H. Ribeiro, M. Boudart, R.A. Dalla Betta, E. Iglesia, Catalytic reactions of n-Alkanes on β-W_2C and WC: The effect of surface oxygen on reaction pathways, Journal of Catalysis, 130 (1991) 498-513.
[7] F.H. Ribeiro, R.A. Dalla Betta, M. Boudart, J. Baumgartner, E. Iglesia, Reactions of neopentane, methylcyclohexane, and 3,3-dimethylpentane on tungsten carbides: The effect of surface oxygen on reaction pathways, Journal of Catalysis, 130 (1991) 86-105.
[8] E. Iglesia, J.E. Baumgartner, F.H. Ribeiro, M. Boudart, Bifunctional reactions of alkanes on tungsten carbides modified by chemisorbed oxygen, Journal of Catalysis, 131 (1991) 523-544.
[9] E. Iglesia, F.H. Ribeiro, M. Boudart, J.E. Baumgartner, Synthesis, characterization, and catalytic properties of clean and oxygen-modified tungsten carbides, Catalysis Today, 15 (1992) 307-337.
[10] T. Wang, Y.-W. Li, J. Wang, M. Beller, H. Jiao, Dissociative Hydrogen Adsorption on the Hexagonal Mo_2C Phase at High Coverage, The Journal of Physical Chemistry C, 118 (2014) 8079-8089.
[11] A.J. Medford, A. Vojvodic, F. Studt, F. Abild-Pedersen, J.K. Nørskov, Elementary steps of syngas reactions on Mo_2C(001): Adsorption thermochemistry and bond dissociation, Journal of Catalysis, 290 (2012) 108-117.
[12] A.S. Rocha, A.B. Rocha, V.T. da Silva, Benzene adsorption on Mo_2C: A theoretical and experimental study, Applied Catalysis A: General, 379 (2010) 54-60.

[13] B. Zhou, X. Liu, J. Cuervo, D. Salahub, Density functional study of benzene adsorption on the α-Mo2C(0001) surface, Struct Chem, 23 (2012) 1459-1466.
[14] X. Liu, A. Tkalych, B. Zhou, A.M. Köster, D.R. Salahub, Adsorption of Hexacyclic C_6H_6, C_6H_8, C_6H_{10}, and C_6H_{12} on a Mo-Terminated α-Mo_2C (0001) Surface, The Journal of Physical Chemistry C, 117 (2013) 7069-7080.
[15] J.-S. Choi, J.-M. Krafft, A. Krzton, G. Djéga-Mariadassou, Study of Residual Oxygen Species over Molybdenum Carbide Prepared During In Situ DRIFTS Experiments, Catalysis Letters, 81 (2002) 175-180.
[16] A. Mehdad, R.E. Jentoft, F.C. Jentoft, Passivation Agents and Conditions for Mo_2C and W_2C: Effect on Catalytic Activity for Toluene Hydrogenation Journal of Catalysis, 347 (2017) 89-101.
[17] M.M. Sullivan, A. Bhan, Acid site densities and reactivity of oxygen-modified transition metal carbide catalysts, Journal of Catalysis, 344 (2016) 53-58.
[18] A. Mehdad, R.E. Jentoft, F.C. Jentoft, Single-phase mixed molybdenum-niobium carbides: Synthesis, characterization and multifunctional catalytic behavior in toluene conversion, Journal of Catalysis, 351 (2017) 161-173.
[19] C.C. Yu, S. Ramanathan, B. Dhandapani, J.G. Chen, S.T. Oyama, Bimetallic Nb-Mo Carbide Hydroprocessing Catalysts:Synthesis, Characterization, and Activity Studies, The Journal of Physical Chemistry B, 101 (1997) 512-518.
[20] A.F. Lamic, C.H. Shin, G. Djéga-Mariadassou, C. Potvin, Characterization of New Bimetallic Oxycarbide ($MoWC_{0.5}O_{0.6}$) for Bifunctional Isomerization of n-Heptane, Catalysis Letters, 107 (2006) 89-94.
[21] L. Leclercq, M. Provost, H. Pastor, J. Grimblot, A.M. Hardy, L. Gengembre, G. Leclercq, Catalytic properties of transition metal carbides: I. Preparation and physical characterization of bulk mixed carbides of molybdenum and tungsten, Journal of Catalysis, 117 (1989) 371-383.
[22] L.A. Bastos, W.R. Monteiro, M.A. Zacharias, G.M. da Cruz, J.A.J. Rodrigues, Preparation and Characterization of Mo/W Bimetallic Carbides by Using Different Synthesis Methods, Catalysis Letters, 120 (2008) 48-55.
[23] S.T. Oyama, C. Charles Yu, S. Ramanathan, Transition Metal Bimetallic Oxycarbides: Synthesis, Characterization, and Activity Studies, Journal of Catalysis, 184 (1999) 535-549.
[24] J.S. Lee, S.T. Oyama, M. Boudart, Molybdenum carbide catalysts: I. Synthesis of unsupported powders, Journal of Catalysis, 106 (1987) 125-133.
[25] H.A. Al-Megren, S.L. Gonzalez-Cortes, T. Xiao, M.L.H. Green, A comparative study of the catalytic performance of Co-Mo and Co(Ni)-W carbide catalysts in the hydrodenitrogenation (HDN) reaction of pyridine, Applied Catalysis A: General, 329 (2007) 36-45.
[26] J.B. Claridge, A.P.E. York, A.J. Brungs, M.L.H. Green, Study of the Temperature-Programmed Reaction Synthesis of Early Transition Metal Carbide and Nitride Catalyst Materials from Oxide Precursors, Chemistry of Materials, 12 (1999) 132-142.
[27] T. Xiao, H. Wang, A.P.E. York, V.C. Williams, M.L.H. Green, Preparation of Nickel-Tungsten Bimetallic Carbide Catalysts, Journal of Catalysis, 209 (2002) 318-330.
[28] T.-C. Xiao, A.P.E. York, H. Al-Megren, C.V. Williams, H.-T. Wang, M.L.H. Green, Preparation and Characterisation of Bimetallic Cobalt and Molybdenum Carbides, Journal of Catalysis, 202 (2001) 100-109.
[29] M. Arbib, E. Silberberg, F. Reniers, C. Buess-Herman, On the synthesis and characterization of mixed (Mo,W) carbides, Journal of the European Ceramic Society, 18 (1998) 1503-1511.
[30] T.H. Nguyen, T.V. Nguyen, Y.J. Lee, T. Safinski, A.A. Adesina, Structural evolution of alumina supported Mo–W carbide nanoparticles synthesized by precipitation from homogeneous solution, Materials Research Bulletin, 40 (2005) 149-157.

[31] A. El-Himri, P. Núñez, F. Sapiña, R. Ibanez, A. Beltran, J.-M.a. Martínez-Agudoc, Synthesis of new molybdenum-tungsten, vanadium-tungsten and vanadium-molybdenum-tungsten oxynitrides from freeze-dried precursors, Journal of Solid State Chemistry, 177 (2004) 2423-2431.
[32] A. El-Himri, F. Sapina, R. Ibanez, A. Beltran, Synthesis of new vanadium-chromium and chromium-molybdenum oxynitrides by direct ammonolysis of freeze-dried precursors, Journal of Materials Chemistry, 10 (2000) 2537-2541.
[33] A. El-Himri, M. Cairols, S. Alconchel, F. Sapina, R. Ibanez, D. Beltran, A. Beltran, Freeze-dried precursor-based synthesis of new vanadium-molybdenum oxynitrides, Journal of Materials Chemistry, 9 (1999) 3167-3171.
[34] X.-H. Wang, M.-H. Zhang, W. Li, K.-Y. Tao, A simple synthesis route and characterisation of Co_3Mo_3C, Dalton Transactions, (2007) 5165-5170.
[35] S. Chouzier, P. Afanasiev, M. Vrinat, T. Cseri, M. Roy-Auberger, One-step synthesis of dispersed bimetallic carbides and nitrides from transition metals hexamethylenetetramine complexes, Journal of Solid State Chemistry, 179 (2006) 3314-3323.
[36] M. Patel, J. Subrahmanyam, Synthesis of nanocrystalline molybdenum carbide (Mo_2C) by solution route, Materials Research Bulletin, 43 (2008) 2036-2041.
[37] C. Giordano, C. Erpen, W. Yao, B. Milke, M. Antonietti, Metal Nitride and Metal Carbide Nanoparticles by a Soft Urea Pathway, Chemistry of Materials, 21 (2009) 5136-5144.
[38] C. Giordano, C. Erpen, W. Yao, M. Antonietti, Synthesis of Mo and W Carbide and Nitride Nanoparticles via a Simple "Urea Glass" Route, Nano Letters, 8 (2008) 4659-4663.
[39] L. Leclercq, M. Provost, H. Pastor, G. Leclercq, Catalytic properties of transition metal carbides: II. Activity of bulk mixed carbides of molybdenum and tungsten in hydrocarbon conversion, Journal of Catalysis, 117 (1989) 384-395.
[40] T. Xiao, A. Hanif, A.P.E. York, J. Sloan, M.L.H. Green, Study on preparation of high surface area tungsten carbides and phase transition during the carburisation, Physical Chemistry Chemical Physics, 4 (2002) 3522-3529.
[41] G. Leclercq, M. Kamal, J.M. Giraudon, P. Devassine, L. Feigenbaum, L. Leclercq, A. Frennet, J.M. Bastin, A. Löfberg, S. Decker, M. Dufour, Study of the Preparation of Bulk Powder Tungsten Carbides by Temperature Programmed Reaction with CH_4+ H_2 Mixtures, Journal of Catalysis, 158 (1996) 142-169.
[42] J.M. Giraudon, P. Devassine, J.F. Lamonier, L. Delannoy, L. Leclercq, G. Leclercq, Synthesis of Tungsten Carbides by Temperature-Programmed Reaction with CH_4–H_2 Mixtures. Influence of the CH_4 and Hydrogen Content in the Carburizing Mixture, Journal of Solid State Chemistry, 154 (2000) 412-426.
[43] A.B. Kehoe, D.O. Scanlon, G.W. Watson, Role of Lattice Distortions in the Oxygen Storage Capacity of Divalently Doped CeO_2, Chemistry of Materials, 23 (2011) 4464-4468.
[44] D.O. Scanlon, B.J. Morgan, G.W. Watson, The origin of the enhanced oxygen storage capacity of $Ce_{1-x}(Pd/Pt)_xO_2$, Physical Chemistry Chemical Physics, 13 (2011) 4279-4284.
[45] L. Volpe, M. Boudart, Compounds of molybdenum and tungsten with high specific surface area: II. Carbides, Journal of Solid State Chemistry, 59 (1985) 348-356.
[46] K.T. Jung, W.B. Kim, C.H. Rhee, J.S. Lee, Effects of Transition Metal Addition on the Solid-State Transformation of Molybdenum Trioxide to Molybdenum Carbides, Chemistry of Materials, 16 (2003) 307-314.
[47] C. Bouchy, S.B. Derouane-Abd Hamid, E.G. Derouane, A new route to the metastable FCC molybdenum carbide α-MoC_{1-x}, Chemical Communications, (2000) 125-126.
[48] P. Delporte, F.d.r. Meunier, C. Pham-Huu, P. Vennegues, M.J. Ledoux, J. Guille, Physical characterization of molybdenum oxycarbide catalyst; TEM, XRD and XPS, Catalysis Today, 23 (1995) 251-267.
[49] W. Xu, P. Ramirez, D. Stacchiola, J. Rodriguez, Synthesis of α-MoC_{1-x} and β-MoC_y Catalysts for CO_2 Hydrogenation by Thermal Carburization of Mo-oxide in Hydrocarbon and Hydrogen Mixtures, Catalysis Letters, 144 (2014) 1418-1424.

[50] T. Xiao, A.P.E. York, K.S. Coleman, J.B. Claridge, J. Sloan, J. Charnock, M.L.H. Green, Effect of carburising agent on the structure of molybdenum carbides, Journal of Materials Chemistry, 11 (2001) 3094-3098.
[51] K.J. Leary, J.N. Michaels, A.M. Stacy, The use of TPD and TPR to study subsurface mobility: Diffusion of oxygen in Mo_2C, Journal of Catalysis, 107 (1987) 393-406.
[52] P.S.F. Mendes, G. Lapisardi, C. Bouchy, M. Rivallan, J.M. Silva, M.F. Ribeiro, Hydrogenating activity of Pt/zeolite catalysts focusing acid support and metal dispersion influence, Applied Catalysis A: General, 504 (2015) 17-28.
[53] V.V. Pushkarev, K. An, S. Alayoglu, S.K. Beaumont, G.A. Somorjai, Hydrogenation of benzene and toluene over size controlled Pt/SBA-15 catalysts: Elucidation of the Pt particle size effect on reaction kinetics, Journal of Catalysis, 292 (2012) 64-72.
[54] J.W. Thybaut, M. Saeys, G.B. Marin, Hydrogenation kinetics of toluene on Pt/ZSM-22, Chemical Engineering Journal, 90 (2002) 117-129.
[55] M. Vasiur Bahaman, M. Albert Vannice, The hydrogenation of toluene and o-, m-, and pxylene over palladium: I. Kinetic behavior and o-xylene isornerization, Journal of Catalysis, 127 (1991) 251-266.
[56] K. Shimizu, T. Sunagawa, C.R. Vera, K. Ukegawa, Catalytic activity for synthesis of isomerized products from benzene over platinum-supported sulfated zirconia, Applied Catalysis A: General, 206 (2001) 79-86.
[57] J. Wang, Q. Li, J. Yao, The effect of metal–acid balance in Pt-loading dealuminated Y zeolite catalysts on the hydrogenation of benzene, Applied Catalysis A: General, 184 (1999) 181-188.
[58] S.J. Ardakani, X. Liu, K.J. Smith, Hydrogenation and ring opening of naphthalene on bulk and supported Mo_2C catalysts, Applied Catalysis A: General, 324 (2007) 9-19.
[59] M. Egorova, R. Prins, Hydrodesulfurization of dibenzothiophene and 4,6-dimethyldibenzothiophene over sulfided NiMo/γ-Al_2O_3, CoMo/γ-Al_2O_3, and Mo/γ-Al_2O_3 catalysts, Journal of Catalysis, 225 (2004) 417-427.
[60] T. Pham, D. Shi, D. Resasco, Kinetics and Mechanism of Ketonization of Acetic Acid on Ru/TiO_2 Catalyst, Top Catal, 57 (2014) 706-714.